



City Research Online

City St George's, University of London

Citation: Vidal Roncero, A., Gavaises, M. & Koukouvinis, P. (2020). Vapor-Liquid Equilibrium calculations at specified composition, density and temperature with the Perturbed Chain Statistical Associating Fluid Theory (PC-SAFT) Equation of State. *Fluid Phase Equilibria*, 521, 112661. doi: 10.1016/j.fluid.2020.112661

This is the accepted version of the paper.

This version of the publication may differ from the final published version. To cite this item please consult the publisher's version.

Permanent repository link: <https://openaccess.city.ac.uk/id/eprint/24214/>

Link to published version: <https://doi.org/10.1016/j.fluid.2020.112661>

Copyright and Reuse: Copyright and Moral Rights remain with the author(s) and/or copyright holders. Copies of full items can be used for personal research or study, educational, or not-for-profit purposes without prior permission or charge, unless otherwise indicated, provided that the authors, title and full bibliographic details are credited, a hyperlink and/or URL is given for the original metadata page and the content is not changed in any way. For full details of reuse please refer to [City Research Online policy](#).

1 Vapor-Liquid Equilibrium calculations at specified
2 composition, density and temperature with the
3 Perturbed Chain Statistical Associating Fluid Theory
4 (PC-SAFT) Equation of State

5 *Alvaro Vidal*, Phoevos Koukouvini, Manolis Gavaises*

6 School of Mathematics, Computer Science & Engineering, Department of Mechanical
7 Engineering & Aeronautics, City University London, Northampton Square EC1V 0HB,
8 United Kingdom

9 *Corresponding author: alvaro.vidal-roncero@city.ac.uk

10 **Keywords:** PC-SAFT, VT-FLASH, VT-STABILITY, Helmholtz energy minimisation

11 **Abstract.** In this study, the PC-SAFT equation of state is used for vapour-liquid equilibrium calculations
12 using as independent variables the mixture composition, density and temperature. The method is based
13 on unconstrained minimisation of the Helmholtz Free energy via a combination of the successive
14 substitution iteration and Newton-Raphson minimisation methods with line-search; the positive
15 definiteness of the Hessian is guaranteed by a modified Cholesky decomposition. The algorithm consists
16 of two stages; initially, the mixture is assumed to be a single-phase and its stability is assessed; in case of
17 being found unstable, a second stage of phase splitting (flash) takes place, in which the pressure of the
18 fluid and compositions of both the liquid and vapor phases are calculated. The reliability of two different

19 methods presented in the existing literature, (i) using mole numbers and (ii) using the logarithm of the
20 equilibrium constants as iterative variables, is evaluated in terms of both iterations and computational
21 time needed to reach convergence, for seven test cases. These include both single and multicomponent
22 Diesel fuel surrogates, known to give incomplete density information when using pressure and
23 temperature as independent variables. Results show that iterating with the logarithm of the equilibrium
24 constants also reproduces this issue, while it requires a smaller number of iterations than using with
25 mole numbers as independent variables. However, the total computational time needed for the latter
26 case is vastly inferior. Pressure and vapor volume fraction fields are discussed for a range of
27 temperatures and densities, apart from the number of iterations needed during the flash calculation
28 stage. A performance comparison is obtained against the Peng-Robinson equation of state, showing
29 similar number of iterations required but a computational time increasing with the number of
30 components. While for a single component PC-SAFT needs around 3 times more CPU time, for 4
31 components it is 6 times and for a mixture of 8 components it increases up to 14 times. Finally, the
32 method is demonstrated to converge unconditionally for all conditions tested.

33 **1 Introduction**

34 The PC-SAFT equation of state (EoS)¹ is a theoretically derived model, based on perturbation theory²⁻⁵,
35 that requires five molecular-based parameters per component for associating fluids and only three for
36 non-associating ones. Several advantages accrue when using the PC-SAFT EoS compared to a cubic EoS
37 to calculate fluid properties. The PC-SAFT EoS more accurately predicts derivative properties, reducing
38 errors by a factor of up to eight^{6,7}, as compared to predictions with a cubic EoS, such as the Peng-
39 Robinson⁸ (PR) or Soave-Redlich-Kwong⁹ (SRK) EoS. Density predictions with the PC-SAFT EoS exhibit six
40 times lower error for a widely used surrogate such as dodecane¹⁰ and half the error of those made with
41 improved cubic equations, such as volume-translated versions¹¹. The PC-SAFT EoS provides satisfactory
42 agreement between calculated and experimental properties of reservoir fluids¹², natural gas¹³ and
43 asphaltene phase behaviour^{14,15}.

44 There is a wide body of research comparing the accuracy of PC-SAFT against other EoS in multiphase
45 problem, not exclusively on vapor-liquid equilibrium. Arya et al.¹⁶ and more recently Vieira de Melo et
46 al.¹⁷ compared the PC-SAFT and Cubic-Plus-Association¹⁸ EoS for phase calculations of asphaltenes
47 present in crude oils where although both EoS gave acceptable results, the authors drew different
48 conclusions. Gong et al.¹⁹ compared Peng Robinson and PC-SAFT EoS while modelling the VLE of mixed
49 refrigerants, with no clear advantage of using one EoS over another. The group of the authors (Vidal et
50 al.²⁰) used it to precisely model the volatility curves of Diesel surrogates up to eight components. Held et
51 al.²¹ modelled the solubility of sugar and sugar alcohols in ionic liquids, with reasonable accuracy.
52 Peyvandi et al.²² compared PC-SAFT, SAFT+CUBIC and PR EoS in the modelling of cryogenic fluids, with a
53 clear disadvantage on the use of PR EoS. Economou et al.²³ investigated the VLE of gaseous mixtures
54 related to carbon dioxide capture technologies using several EoS: SRK, PR, SAFT, and PC-SAFT EoS,
55 among them PC-SAFT showed to be the most accurate when no binary interaction parameters (BIP) are
56 used, although comparable accuracy was observed with a fitted BIP. However, most of the studies focus
57 on the modelling of the phase equilibria as 'static' problems, without considering flowing systems,
58 where the VLE problem is only part of the whole framework of Computational Fluid Dynamics
59 simulations. Exceptions can be found on the latest work in Diesel sprays²⁴ or Diesel injections²⁵, however
60 the fuel in these two cases is a single component or a pseudo-component and various techniques are
61 used to work around the problem of density undefinition inside the saturation curve. Overall, there
62 seems to be evidence to indicate that independent variables other than pressure and temperature are
63 needed for complex computational fluid dynamics simulations.

64 The use of flash with density (or specific volume), temperature and composition is particularly useful
65 whenever the pressure is unknown in an enclosed fluid and the phase change is a possibility. This
66 happens in storage tanks design, during the capturing process of acid gases within oil reservoirs, or
67 compositional reservoir simulations as there is no balance equation for pressure²⁶. Also, in most real
68 fluid equations of state, e.g. PC-SAFT or cubic EoS, the formulation is given depending naturally on
69 density, or volume, temperature and composition, which also makes the choice of these variables for

70 the VLE calculations the most straight-forward. However, the existing body of research has only
71 employed pressure and temperature as independent variables for vapor-liquid equilibrium calculations
72 (PT-VLE) with the PC-SAFT EoS. Moreover, this method shows its limitations when the phase change is at
73 constant temperature and pressure, characteristic of single components. At constant pressure and
74 temperature, the state of the substance is undetermined at saturation conditions. However, the volume
75 (or density) changes provide the complete information. Lastly, this undefinition is not restricted only to
76 single components as it also appears in multicomponent mixtures for three phase systems²⁷ and those
77 composed of similar components, as will be shown in the results section for a Diesel surrogate.

78 A seminal study in this area is the one of Michelsen²⁸, who proposed the use of volume and
79 temperature as independent variables and the minimising the Helmholtz Free energy rather than the
80 Gibbs free energy for the multiphase problem. In addition, for pressure-explicit EoS this approach would
81 also avoid the need for an iterative process to find the density from pressure, as the pressure becomes
82 then an output of the minimisation process. This approach was then implemented for the stability
83 testing of hydrocarbon mixtures²⁹ using the SRK and the PR EoS with the tunnelling method³⁰. Following
84 work used the successive substitution iteration (SSI) method and the PR EoS for the flash problem³¹.
85 Over the past decade, studies related to minimising the Helmholtz free energy have been focused on
86 the Newton method³². Moreover, new frameworks have been published using variations of the
87 independent variables or decoupling the pressure equality condition during the flash stage³³. Recently, a
88 framework using constrained minimisation has been also published Paterson et al.³⁴ in a generalized
89 form for specifications based on state functions other than pressure and temperature. There have been
90 works using density and temperature as independent variables for the calculation of the saturation
91 curves of single components in PC-SAFT^{35, 36}. However, to author's best knowledge, stability analysis and
92 flash calculations using the this equation of state have been restricted to temperature T and pressure P
93 as independent variables³⁷.

94 Following the above limitation when pressure and temperature are used as independent variables,
95 the novelty of this work is the provision and assessment of the necessary numerical framework using

96 composition, density and temperature as input variables for the calculation of the vapor-liquid
97 equilibrium within the structure of PC-SAFT, via the unconstrained minimisation of the Helmholtz Free
98 energy.

99 In this study, the minimum of the molar Helmholtz Free energy A is calculated, defined in terms of
100 density ρ , temperature T and composition \mathbf{z} as:

$$101 \quad A(\mathbf{z}, \rho, T) = \sum_{i=1}^{nc} z_i A_i^{id}(P(\mathbf{z}, \rho, T), T) + A^{res}(\mathbf{z}, \rho, T) \quad (1)$$

102 Where the superscripts *id* and *res* refer to the ideal, given by the fundamental gas relation, and
103 residual contributions of the Helmholtz Free Energy, modelled by PC-SAFT, respectively. This
104 optimisation problem is solved via a combination of the successive substitution iteration (SSI) and the
105 Newton minimisation method with a two-step line-search procedure, and the positive definiteness of
106 the Hessian is guaranteed by a modified Cholesky decomposition³⁸. The algorithm consists of two
107 stages: first, the mixture is assumed to be in a single phase state and its stability is assessed via the
108 minimisation of the Tangent Plane Distance (TPD); in case the minimum of the TPD is found to be
109 negative, the mixture is considered unstable and a second stage of flash, i.e. phase splitting, takes place
110 consisting on the search for the global minimum of the Helmholtz Free Energy. As a result, the pressure
111 of the fluid and the compositions of both the liquid and vapor phases are calculated, from which every
112 other thermodynamic property can be calculated, i.e. internal energy, enthalpy, entropy, speed of
113 sound, etc, using the PC-SAFT¹. The reliability of two different methods for the flash stage, NVL³⁹ and
114 $\ln K$ ³³, are evaluated in terms of both iterations and computing time needed to reach convergence.
115 Following the work of von Solmons et al in VLE calculations⁴⁰, this work also assesses the computational
116 time needed for its completion. The robustness of the algorithm is then tested with a mixture of 50
117 components and several other examples often found in the literature in two-phase equilibrium
118 calculations. Particular attention is paid to the case of a single component and a Diesel surrogate, known
119 to reproduce the already highlighted incomplete density information when using pressure and

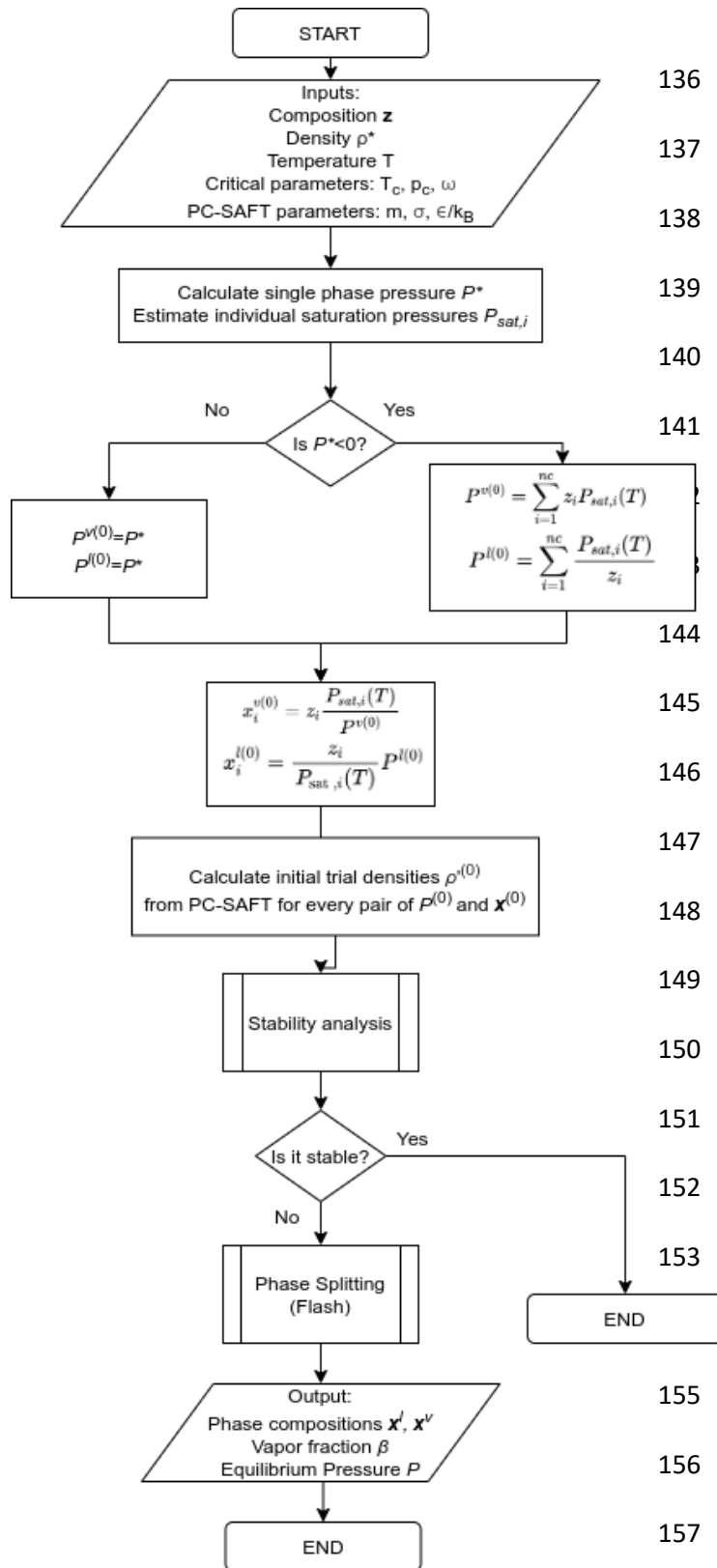
120 temperature as independent variables. The overall accuracy of the VT-VLE algorithm combined with PC-
121 SAFT is tested against experimental data for a selected number of examples.

122

123 Following the above introduction, the second section provides the theoretical framework, describing
124 the Newton method, the stability and flash stages, the strategy followed for the initialisation, the initial
125 phase splitting in case the mixture is found unstable. The third section shows the results obtained for 7
126 test cases, providing the number of iterations and the computational time needed for convergence for
127 both the NVL and lnK methods. Then, the pressure and vapor volume fraction fields for selected
128 examples are discussed for a range of temperatures and densities, apart from the number of iterations
129 needed for convergence during the flash stage. A performance comparison is obtained against Peng-
130 Robinson, showing a substantial decrease in computational time when using the cubic than using the
131 molecular based EoS. Finally, validation cases against experiments are provided before concluding. The
132 Supplementary Information provides detailed information regarding the components used in this study
133 and the analytical derivatives needed for the algorithm.

134

135 **2 Method**



136 Any isolated system at constant
 137 density and temperature tends
 138 spontaneously to an equilibrium state
 139 while decreasing the Helmholtz free
 140 energy of the system, until the global
 141 minimum is reached, i.e. equilibrium.
 However, it may be the case that the
 state at which the equilibrium occurs is
 144 that of vapor and liquid coexisting.
 145 Thus, the amount of each phase, their
 146 composition and pressure need to be
 147 calculated.
 148 In this work, the presented
 149 algorithm studies the stability of the
 150 homogeneous mixture using the PC-
 151 SAFT EoS for a given composition
 152 z_1, \dots, z_{nc} with density ρ and at a certain
 153 temperature T ; in case it is found to be
 unstable, the vaporized fraction of the
 155 substance, the compositions of both
 156 phases and the resulting pressure in
 157 equilibrium are calculated via flash.

Scheme 1. General diagram for multiphase calculations

Both algorithms for the stability and

159 flash stages have been already developed and published for the Peng Robinson EoS; only minor changes
 160 are needed for the PC-SAFT EoS regarding the convergence criteria in the iterations and constraints.

161 Scheme 1 shows the general diagram of the algorithm used in the multiphase calculations. For
162 consistency, the whole algorithm is described here, and any novelty introduced is clearly stated in the
163 following subsections.

164 2.1 Newton method

165 The Newton method⁴¹ provides a good approximation for the root of an objective function.

166 Essentially, the independent variables vector ϵ of the objective function is iteratively updated from step
167 k to the following $k + 1$ by

$$168 \quad \epsilon^{(k+1)} = \epsilon^{(k)} + \lambda \mathbf{p}^{(k)} \quad (2)$$

169 where λ is the step length, which defines how far the next step moves along the Newton direction $\mathbf{p}^{(k)}$.

170 The step length is set in two stages. First, an initial value of 1 is given and it is continuously halved until

171 $\epsilon^{(k+1)}$ satisfies the variable constraints of each problem, specified in the following sections. These

172 constraints may be related, for instance, to the feasible values of density or compositions. Then, an

173 inexact line search is executed to obtain a step length that satisfies the Wolfe conditions⁴², which gives

174 an efficient decrease of the objective function.

175 The Newton direction $\mathbf{p}^{(k)}$ is calculated by solving the system of equations:

$$176 \quad \mathbf{H}^{(k)} \mathbf{p}^{(k)} = -\mathbf{g}^{(k)} \quad (3)$$

177 where \mathbf{g} and \mathbf{H} are the gradient and Hessian of the objective function to be minimised. In case the use

178 of successive substitution iterations (SSI) method is needed, the only difference with the Newton

179 method is that the Hessian is equal to the identity matrix \mathbf{I} .

180 For the system (3) to have a solution, the Hessian \mathbf{H} needs to be positive definite, i.e. its eigenvalues

181 are all positive real numbers. To satisfy this condition, the modified Cholesky factorisation³⁸ is applied in

182 this study. The modifications introduce symmetric interchanges of rows and columns, via a permutation

183 matrix \mathbf{P} , and the addition of a non-negative diagonal matrix \mathbf{E} which is zero if the Hessian \mathbf{H} is positive.

184 Therefore, the system of equations (3) gets transformed, for every iteration step k , into:

$$185 \quad [\mathbf{P}(\mathbf{H} + \mathbf{E})\mathbf{P}^T](\mathbf{P}\mathbf{p}) = -\mathbf{P}\mathbf{g} \quad (5)$$

186 Once the positive definiteness of the modified Hessian is satisfied, it is factorised as:

$$187 \quad \mathbf{P}(\mathbf{H} + \mathbf{E})\mathbf{P}^T = \mathbf{M}\mathbf{M}^T \quad (6)$$

188 where \mathbf{M} is a lower triangular matrix. Finally, the system is solved by performing backward and
189 forward

190 substitution with the triangular matrix, which consists in the following sequence of operations:

191 1. Solve $\mathbf{M}\mathbf{u} = -\mathbf{P}\mathbf{g}$ to obtain \mathbf{u} .

192 2. Solve $\mathbf{M}^T\tilde{\mathbf{u}} = \mathbf{u}$ to obtain $\tilde{\mathbf{u}}$.

193 3. Calculate the gradient $\mathbf{g} = \mathbf{P}^T \tilde{\mathbf{u}}$.

194 Convergence criteria

195 The Newton method is assumed to have converged whenever one of the following criteria is
196 achieved:

197 1. The Euclidean norm of the change in the iteration variables $\|\lambda\mathbf{p}\|^2$ is less than 10^{-7} .

198 2. The Euclidean norm of the gradient $\|\mathbf{g}\|^2$ is less than 10^{-10} .

199 2.2 Stability stage

200 The stability problem is solved in a similar fashion as that presented by Baker et al.^{43f} for a mixture at
201 constant temperature T and pressure P . A homogeneous mixture at a certain temperature T is in a
202 stable state if the tangent plane to the Helmholtz free energy surface at composition z and density ρ
203 does not intersect the Helmholtz free energy surface at any other point. The stability is tested by
204 purposely dividing the homogeneous mixture in two phases, one of them in an infinitesimal amount and
205 it is referred to as 'trial phase'. For any feasible two-phase mixture, if a decrease in the Helmholtz free
206 energy is not achieved, then the mixture is stable. The so-called tangent plane distance (TPD) as function
207 of the density times the composition of the trial phase $\rho'x_i'$ is:

$$208 \quad TPD(\rho'x_i') = -\frac{P'-P^*}{R_gT} + \sum_{i=1}^{nc} \rho'x_i'(\log f_i' - \log f_i^*) \quad (7)$$

209 where the tildes over the variables indicate those calculated at the trial conditions and the asterisk
210 indicates those calculated at the feed conditions. R_g is the universal gas constant and f_i is the fugacity of

211 the component i . Within the structure of PC-SAFT, it is advisable to write the expression in terms of the
 212 residual reduced Helmholtz free energy, having then:

$$213 \quad P = \left(1 + \rho_m \frac{\partial a^{res}}{\partial \rho_m} \right) k_B T \rho_m \left(10^{10} \frac{\text{\AA}}{m} \right)^3 \quad (8)$$

214 Where ρ_m is the number density of molecules and k_B is the Boltzmann constant. Regarding the
 215 fugacity,

$$216 \quad \log f_i = \log(x_i P \phi_i) \quad (9)$$

217 Where the logarithm of the fugacity coefficient ϕ of the component i is defined as:

$$218 \quad \log \phi_i = \frac{1}{R_g T} \left(\frac{\partial A^r}{\partial N_i} \right)_{T, V, N_s \neq i} - \log Z \quad (10)$$

219 where Z is the compressibility factor and A^r is the non-reduced Helmholtz free energy. This equation is
 220 used for the Peng Robinson EoS following the formulation of Nichita³³. For PC-SAFT, the original
 221 formulation of Gross and Sadowski¹ is used:

$$222 \quad \log \phi_i = a^{res} + \rho_m \frac{\partial a^{res}}{\partial \rho_m} + \frac{\partial a^{res}}{\partial x_i} - \sum_{j=1}^{nc} x_j \frac{\partial a^{res}}{\partial x_j} \quad (11)$$

223 The derivation of the TPD function can be seen in the work of Mikyska and Firoozabadi⁴⁴. The stability
 224 is assured if for any feasible solution $\rho' x_i'$ the TPD function is non-negative. Therefore, the problem is
 225 reduced to the search of the global minima of the TPD function, subjected to the material constraints:

$$226 \quad \rho' x_i' > 0 \quad \forall i \quad (12)$$

$$227 \quad \sum_{i=1}^{nc} \rho' x_i' \leq \rho_{max}(x_i', T) \quad (13)$$

228 where ρ_{max} refers to the maximum packing fraction at fixed composition x_i' and temperature T . For
 229 the Newton method, the required gradient is given by:

$$230 \quad \frac{\partial TPD}{\partial (\rho' x_i')} = \log f_i' - \log f_i^* \quad (14)$$

231 Nichita⁴⁵ studied alternatives to use as iteration variables such as $\log(\rho' x_i')$ and $\alpha_i = 2\sqrt{\rho' x_i'}$, in a
 232 similar manner as shown by Michelsen²⁸. His study concluded that the α_i ensured the most robust and

233 fast convergence for the stability problem and it is the one used in this work. For this case, the gradient
 234 is:

$$235 \quad \frac{\partial TPD}{\partial \alpha_i} = \sqrt{\rho' x_i} (\log f_i' - \log f_i^*) \quad (15)$$

236 and the Hessian is:

$$237 \quad \frac{\partial TPD}{\partial \alpha_i \partial \alpha_j} = \delta_{ij} + \sqrt{\rho' x_i} \sqrt{\rho' x_j} \left[\frac{\partial \log f_i}{\partial n_j} - \frac{\delta_{ij}}{\rho' x_i} \right] \quad (16)$$

238 In order to avoid unnecessary iterations when the Newton is converging to a trivial solution, i.e. $TPD =$
 239 0 , in this work another stopping criterion is used, also first introduced but for the TPN case by
 240 Michelsen²⁸. At every iteration the convergence variable r is checked:

$$241 \quad r = \frac{2 TPD^{(k)}}{\sum_{i=1}^{nc} (\rho' x_i - \rho z_i) (\log f_i' - \log f_i^*)} \quad (17)$$

242 which tends to 1 as the method converges to the trivial solution. Therefore, the iterations are stopped
 243 if $|r - 1| < 0.2$ and $TPD^{(k)} < 10^{-3}$.

244 **2.3 Initialisation**

245 The stability stage needs an initial condition to start the iterative process. Typically, Wilson's
 246 correlation⁴⁶ is used to guess the initial equilibrium constants K_i :

$$247 \quad K_i = \frac{P_{c,i}}{P} \exp \left[5.37(1 + \omega_i) \left(1 - \frac{T_{c,i}}{T} \right) \right] \quad (18)$$

248 where for every component i , $P_{c,i}$ and $T_{c,i}$ are the critical pressure and temperature and ω_i is the
 249 acentric factor. These three values are used in most cubic EoS and are widely available in the literature,
 250 but not in PC-SAFT EoS. However, the exact critical values specific for the PC-SAFT EoS can be calculated
 251 following a published algorithm⁴⁷, which comprises an iterative process in order to verify the three
 252 critical specifications:

$$253 \quad P(T_c, \rho_c) - P_c = 0 \quad (19)$$

$$254 \quad \frac{\partial P}{\partial \rho} = 0 \text{ at } (T_c, \rho_c) \quad (20)$$

255
$$\frac{\partial^2 P}{\partial \rho^2} = 0 \text{ at } (T_c, \rho_c) \quad (21)$$

256

257 Unlike for the PT-multiphase problem, the pressure of the mixture is unknown a-priori for VT
 258 specifications, so a different strategy must be used, as the one used by Nichita⁴⁵. According to Raoult's
 259 law:

260

261
$$K_i = \frac{P_{sat,i}(T)}{P} \quad (22)$$

262 where $P_{sat,i}(T)$ is the saturation pressure of the component i at a temperature T . From this law, follows
 263 that $P_{sat,i}(T) = P$ when $K_i = 1$, therefore from eq. (13) it follows:

264

265
$$P_{sat,i}(T) = P_{c,i} \exp \left[5.37(1 + \omega_i) \left(1 - \frac{T_{c,i}}{T} \right) \right] \quad (23)$$

266 The strategy for the initial composition of the trial phase is slightly different if it is considered to be
 267 vapor-like or liquid-like. Michelsen²⁸ proposed the initial composition of the trial phase, for both cases,
 268 to be:

269
$$x_i^{v(0)} = z_i K_i^{(0)} \quad \text{and} \quad x_i^{l(0)} = \frac{1}{z_i K_i^{(0)}} \quad (24)$$

270 which, using Raoult's law (14) transform to:

271
$$x_i^{v(0)} = z_i \frac{P_{sat,i}(T)}{P^{v(0)}} \quad \text{and} \quad x_i^{l(0)} = \frac{z_i}{P_{sat,i}(T)} P^{l(0)} \quad (25)$$

272 where the initial pressures $P^{v(0)}$ and $P^{l(0)}$ are first taken as that given by the EoS for the single
 273 phase system at T , ρ and composition \mathbf{z} . If the calculated pressure is negative, Mikyska and Firoozabadi
 274⁴⁴ estimated them as:

275

276
$$P^{v(0)} = \sum_{i=1}^{nc} z_i P_{sat,i}(T) \quad \text{and} \quad P^{l(0)} = \sum_{i=1}^{nc} \frac{P_{sat,i}(T)}{z_i} \quad (26)$$

277 The initial density of the trial phase is then calculated iteratively using the EoS for both initial
 278 compositions $x_i^{v(0)}$ and $x_i^{l(0)}$ at fixed temperature T and at the corresponding initial pressures $P^{v(0)}$ and

279 $p^{l(0)}$. As there may be two densities for every composition and pressure, there can be up to 4 initial
 280 estimates; all the initial estimates are used in the stability stage.

281 **2.4 Initial Phase splitting**

282 In case the mixture is found to be unstable, an initial splitting of the homogeneous phase is executed.
 283 From the stability analysis, the composition and density of the trial phase are fixed to ρ' and x'_i . With
 284 variations with respect to the method shown by Jindrova and Mikyska³², the initial density and
 285 composition of the second phase, i.e. ρ'' and x''_i , are estimated in terms of the molar fraction of the trial
 286 phase over the feed, $\beta = N'/N^*$, from the material and volume constraints:

$$287 \quad \beta x'_i + (1 - \beta)x''_i = z_i \quad (27)$$

$$288 \quad \beta \frac{1}{\rho'} + (1 - \beta) \frac{1}{\rho''} = \frac{1}{\rho} \quad (28)$$

289 The initial amount of each phase is estimated in the following way:

290 1. An arbitrary initial trial molar fraction β is chosen. In two phase systems, $\beta \in (0,1)$, thus the
 291 chosen initial value in this work is 0.99.

292 2. The composition and density of the second phase are calculated from the material and volume
 293 constraints (19) (20) by:

$$294 \quad x''_i = \frac{z_i - \beta x'_i}{1 - \beta} \quad (29)$$

295 and

$$296 \quad \rho'' = \frac{1 - \beta}{\frac{1}{\rho} - \beta \frac{1}{\rho'}} \quad (30)$$

297 3. The density of the second phase is checked to be lower than that given by the maximum packing
 298 fraction

$$299 \quad \rho'' < \rho_{max}(x''_i, T) \quad (31)$$

300 If not, a new lower molar fraction value is assumed (i.e. halving the previous value), and the algorithm
 301 returns to step 2.

302 4. The variation in the Helmholtz free energy is calculated by:

303
$$\Delta A = A^{2\ phase} - A^* = (A'(x', \rho', T) + A''(x'', \rho'', T)) - A^* \quad (32)$$

304 5. It is checked whether $\Delta A < 0$, meaning that the current phase split produces a decrease in the
305 Helmholtz free energy. If $\Delta A \geq 0$ the molar fraction is halved and step 2 is repeated. If $\Delta A < 0$ the
306 process is stopped, and the flash stage begins. The phase with the highest density is considered to be
307 the liquid phase (*l*) and the other one the vapor phase (*v*).

308

309

310 2.5 Flash stage

311 Following the initial phase splitting, the flash stage calculates the amount and compositions of both
312 phases in equilibrium, in addition to the final equilibrium pressure. This calculation is done via the
313 minimisation of the variation of the Helmholtz free energy, as in equation 24. Depending on the
314 iteration variables, two methodologies have been tested. Firstly, the one described by Jindrova and
315 Mikyska³⁹ uses the number of moles in both phases and the phase volumes. Secondly, the one
316 described by Nichita³³ uses the natural logarithm of the equilibrium constants. The two methods have
317 been coupled with the PC-SAFT framework and the derivatives needed can be found in the
318 Supplementary Information.

319 Number of moles and volume as iteration variables

320 When using the number of moles and the volume of both phases, per mole of feed, the problem
321 comprises $(2nc)+2$ iteration variables $n_1^v, \dots, n_{nc}^v, V^v, n_1^l, \dots, n_{nc}^l, V^l$. However, because of the material
322 and volume balances:

323

$$324 \quad n_i^v + n_i^l = z_i \quad (33)$$

$$325 \quad V^v + V^l = \frac{1}{\rho} \quad (34)$$

326 the variables of one phase are dependent on those of the other phase. Therefore, as described by
327 Jindrova and Mikyska³⁹, it is possible to solve a reduced system in terms of the $nc+1$ vapor variables. For
328 the reduced problem, the gradient of the system is given by:

$$329 \quad g_i = \frac{\partial \Delta A}{\partial n_i^v} = \frac{\log f_i^v - \log f_i^l}{\sqrt{2}} \quad \text{for } i = 1, nc \quad (35)$$

$$330 \quad g_{nc+1} = \frac{\partial \Delta A}{\partial V^v} = -\frac{P^v - P^l}{\sqrt{2}R_gT} \quad (36)$$

331 and the Hessian:

332
$$\mathbf{H} = 1/2 \begin{pmatrix} & \mathbf{B} & & \vdots & \mathbf{C} \\ & & & \vdots & \\ \dots & \dots & \dots & \vdots & \dots \\ \mathbf{C}^T & & & \vdots & \mathbf{D} \end{pmatrix} \quad (37)$$

333 Where

334
$$B_{ij} = \frac{\partial \log f_i^v}{\partial n_j^v} + \frac{\partial \log f_i^l}{\partial n_j^l} \quad (38)$$

335
$$C_i = - \frac{\frac{\partial P^v}{\partial n_i^v} + \frac{\partial P^l}{\partial n_i^l}}{R_g T} \quad (39)$$

336
$$D = - \frac{\frac{\partial P^v}{\partial V^v} + \frac{\partial P^l}{\partial V^l}}{R_g T} \quad (40)$$

337 In order to obtain the variation of the variables for both phases, the Newton direction ρ is
 338 transformed back into the full $(2nc)+2$ dimension premultiplicating by the reducing matrix \mathbf{Z} :

339
$$\mathbf{Z} = \frac{1}{\sqrt{2}} \begin{pmatrix} I_{nc+1} \\ -I_{nc+1} \end{pmatrix} \quad (41)$$

340 Finally, the composition and density of both phases are calculated by first obtaining the vapor mole
 341 fraction $\beta = \sum_{i=1}^{nc} n_i^v$ and then:

342
$$x_i^v = \frac{n_i^v}{\beta} \quad \text{and} \quad x_i^l = \frac{n_i^l}{1 - \beta} \quad (42)$$

344
$$\rho^v = \frac{\beta}{V^v} \quad \text{and} \quad \rho^l = \frac{1-\beta}{V^l} \quad (43)$$

345 Following the work of Paterson et al.³⁴, the effect of initial Successive Substitution Iterations
 346 (SSI) during the flash stage were tested. However, no improvement was observed and on average more
 347 iterations were needed to reach convergence.

348 **Logarithm of equilibrium constants $\log K_i$ as iteration variables**

349 The use of the logarithms of equilibrium constants, $\log K_i = \log(x_i^v/x_i^l)$, as iteration variables in the
 350 flash problem is one of the most used methods when the multiphase problem is defined in terms of
 351 pressure and temperature. Nichita³³ applied it to the VT-Flash problem by decoupling the pressure

352 equality condition $P^v(x_i^v, \rho^v, T) = P^l(x_i^l, \rho^l, T) = P^{eq}$, which is calculated at every iteration step.

353 Therefore, the iteration variables are reduced to the nc components defining $\log K$. Then, at every step

354 the Rachford-Rice equation is solved to obtain the vapor mole fraction β using the Newton-Raphson

355 method:

$$356 \quad \sum_{i=1}^{nc} \frac{z_i(K_i-1)}{1+\beta(K_i-1)} = 0 \quad (44)$$

358 Which allows to obtain the molar fractions of both phases for every iteration k by:

$$359 \quad x_i^l = \frac{z_i}{1 + \beta(K_i - 1)} \quad (45)$$

360 and

$$361 \quad x_i^v = K_i x_i^l \quad (46)$$

362 Then, the equilibrium pressure P^{eq} is calculated iteratively by solving the volume distribution

363 equation:

$$364 \quad \beta \frac{1}{\rho^v(x_i^v, P^{eq}, T)} + (1 - \beta) \frac{1}{\rho^l(x_i^l, P^{eq}, T)} = \frac{1}{\rho} \quad (47)$$

366 When calculating the density at certain pressure, many roots may be encountered. In such a case, the

367 density giving the least Gibbs free energy is chosen. The iterative method chosen is that of Brent⁴⁸. The

368 gradient in this case reads:

$$369 \quad \frac{\partial \Delta A}{\partial \log K_i} = \log f_i^v - \log f_i^l \quad (48)$$

371 and the Hessian:

$$372 \quad H_{ij} = \frac{\partial \log K_i}{\partial N_j^v} + \frac{\partial \log f_i^v}{\partial N_j^v} + \frac{\partial \log f_i^l}{\partial N_j^l} + \frac{1}{R_g T} \frac{\left(\frac{\partial P^v}{\partial N_i^v} + \frac{\partial P^l}{\partial N_i^l} \right) \left(\frac{\partial P^v}{\partial N_j^v} + \frac{\partial P^l}{\partial N_j^l} \right)}{\frac{\partial P^v}{\partial V^v} + \frac{\partial P^l}{\partial V^l}} \quad (49)$$

373

374 As proposed in the original paper of Nichita³³, a first iteration using the SSI method is applied.

375 **3 Results and Discussion**

376 In this section, results for the VLE problem using composition, density and temperature are shown for
377 a set of seven cases. Case 1 is a single component Diesel surrogate, (n-dodecane) widely used in the
378 Diesel industry; this case will show the performance of the algorithm for single components where the
379 PT FLASH fails. Cases 2 and 3 are binary mixtures, typically used as benchmark cases for testing
380 multiphase equilibrium algorithms³¹. The composition for Case 2 is 0.547413 methane and 0.452587
381 pentane, while for Case 3 is 0.547413 carbon dioxide and 0.452587 decane. Case 4 is another binary
382 mixture used in the widely used database of the so-called 'Spray A'⁴⁹, 0.3 nitrogen and 0.7 dodecane.
383 Case 5 is a four-component mixture, also widely used for testing of multiphase algorithms³¹, composed
384 of 0.2463 nitrogen, 0.2208 methane, 0.2208 propane and 0.3121 decane. Case 6 is a hydrocarbon eight-
385 component mixture created also as a Diesel fuel surrogate⁵⁰, composed of 0.202 octadecane, 0.027
386 hexadecane, 0.292 heptamethylnonane, 0.144 1-methylnaphthalene, 0.154 tetralin, 0.055 trans-decalin,
387 0.051 butylcyclohexane and 0.075 1,2,4-trimethylbenzene. Finally, case 7 explores the application of the
388 presented method to a multi-component mixture consisting of 50 different hydrocarbons, with equally
389 distributed composition ranging from methane to octadecane. The complete set of hydrocarbons is
390 given in the Supplementary Information. Cases 3 and 4 are validated against experiments, apart from an
391 additional synthetic mixture of 6 components, commonly named Y8⁵¹. For all cases, the EoS parameters
392 and binary interaction parameters are given in the Supplementary Information. Table 1 shows the
393 density-temperature grids studied for each case, apart from the number of total points tested with the
394 algorithms.

395 A summary of the iterations needed for convergence for every stage and flash methodologies used in
396 this work can be found in Table 2. The average values are calculated as the sum of the iterations needed
397 until convergence for the whole domain and then divided for the number of points studied. As seen in
398 the first row, the stability analysis grows with the number the components of the mixture. While for a
399 single component (Case 1), the number of iterations needed for convergence in stability is around 4, for
400 binary mixtures (Cases 2-4), it increases to around 7. For the 4 components mixture (Case 5), the

401 number of stability iterations needed are not much affected with respect to the binary mixtures. For the
 402 eight-component hydrocarbon mixture (Case 6), the average number of iterations needed grows around
 403 50%. Finally, for the 50-component mixture (Case 7), the number of iterations is higher but close to the
 404 previous case.

Case	nc	$T(K)$ window	$T(K)$ no. points	ρ (Kmol/m ³) window	ρ no. points	Total no. points
1	1	[280-700]	400	[0.001-5]	400	160000
2	2	[320-430]	110	[0.001-12]	1200	132000
3	2	[250-600]	350	[0.001-9]	900	315000
4	2	[250-650]	400	[0.001-10]	900	360000
5	4	[250-600]	350	[0.001-12]	1200	420000
6	8	[300-750]	450	[0.001-4.5]	450	202500
7	50	[300-650]	400	[0.001-6]	400	160000

Table 1: Density-Temperature window and total number of points.

405 A case dependant result is found for the flash stage. For the NVL method (second row of Table 2), the
 406 binary mixture of Case 2 is the one with the lower number of flash iterations needed, followed by the
 407 single component Case 1 and the other two binary mixture Cases 3 and 4. A substantial increase is found
 408 for the 4-component mixture, which almost triples the iterations needed for the binary mixtures.

409 Although doubling the number of components in Case 6, for the 8-component the flash iterations gets
 410 reduced by 10 for the conditions to converge. Finally, the 50-component mixture shows a doubled
 411 number of iterations with respect to Case 6, needing on average around 30 iterations until convergence
 412 during the flash stage.

413 In the case of the lnK method (third row on Table 2), the number of iterations is significantly reduced
 414 by more than 40% with respect to the NVL method. However, as explained in the methodology section
 415 for the lnK independent variables, this method suffers from the same limitation of the PT-Flash problem

416 and it can't be used for single components and mixtures of similar components, as Cases 1 and 6.
 417 Regarding the rest of cases, Case 2 is the one with the least iterations needed (up to 4), followed by the
 418 other binary mixtures Cases 4 and 3. For Case 5, the 4-component mixture needs between 3 and 4 times
 419 more iterations than for the binary mixtures. For the 50-component surrogate, the difference between
 420 the methods gets reduced to only 2 iterations less than those needed for the NVL-VLE algorithm.

	Case 1	Case 2	Case 3	Case 4	Case 5	Case 6	Case 7
Stability	3.93	7.63	6.26	6.87	11.25	15.31	17.82
Flash (NVL)	7.24	6.26	9.05	9.21	26.82	16.20	30.80
Flash (InK)	-	3.99	5.32	4.24	15.12	-	28.33

421 Table 2: Average number of iterations needed for convergence using every method studied here for
 422 both the stability and flash algorithms.

423 Table 3 shows the average total convergence time, i.e. both stability and flash stages, for any ρ and T
 424 conditions, in ms. The CPU used during this study was an Intel(R) Xeon(R) CPU E5-2690 v3 at 2.60GHz
 425 and a memory of 128GB of RAM. From the number of iterations, it would seem clear that the InK
 426 method was the best one to be used in processes needing fast but reliable calculations, such as those
 427 needed in CFD simulations. However, the time needed for convergence clearly points in the opposite
 428 way, as the InK method lasts a minimum of 20 times longer than the time needed for convergence with
 429 the NVL. This difference in computational time is caused during the calculation of density in the pressure
 430 equality condition, as it needs to be obtained iteratively, while NVL only satisfies it once convergence is
 431 reached. For the single component Case 1, the NVL method needed 0.6 ms, while no results could be
 432 obtained for the InK method as it fails. For the binary mixtures (Cases 2-4), around 1 ms was needed for
 433 the NVL method against the 20-25ms for the InK. The computational time needed for the 4-component
 434 mixture of Case 5 was around 5ms for the NVL method and 135ms for the InK method (25 times longer).
 435 Case 6 needed 15.6 ms with NVL while the InK method failed to converge to the correct solution
 436 whenever the phase transition was isobaric-isothermal. For the 50-components mixture of Case 7, each
 437 complete VLE calculation took close to 2 seconds, while for the InK flash procedure it took 10 times
 438 longer. Therefore, the NVL method is chosen in the following sections.

Flash strategy	Case 1	Case 2	Case 3	Case 4	Case 5	Case 6	Case 7
----------------	--------	--------	--------	--------	--------	--------	--------

NVL	0.68965	1.0782	1.1203	0.77236	7.2450	35.401	1,955
lnK	-	19.933	24.141	23.72	135.48	-	18,378

439 Table 3: Average time, in ms, per case needed for convergence using both flash methods studied here.

440 In the following subsections, results from using NVL iterations are shown regarding the pressure field,
441 vapor volume fraction and number of flash iterations for convergence. Finally, results are validated
442 against experimental VLE data. All the calculation data can be found in the supplementary information.

443 **3.1 Pressure Field**

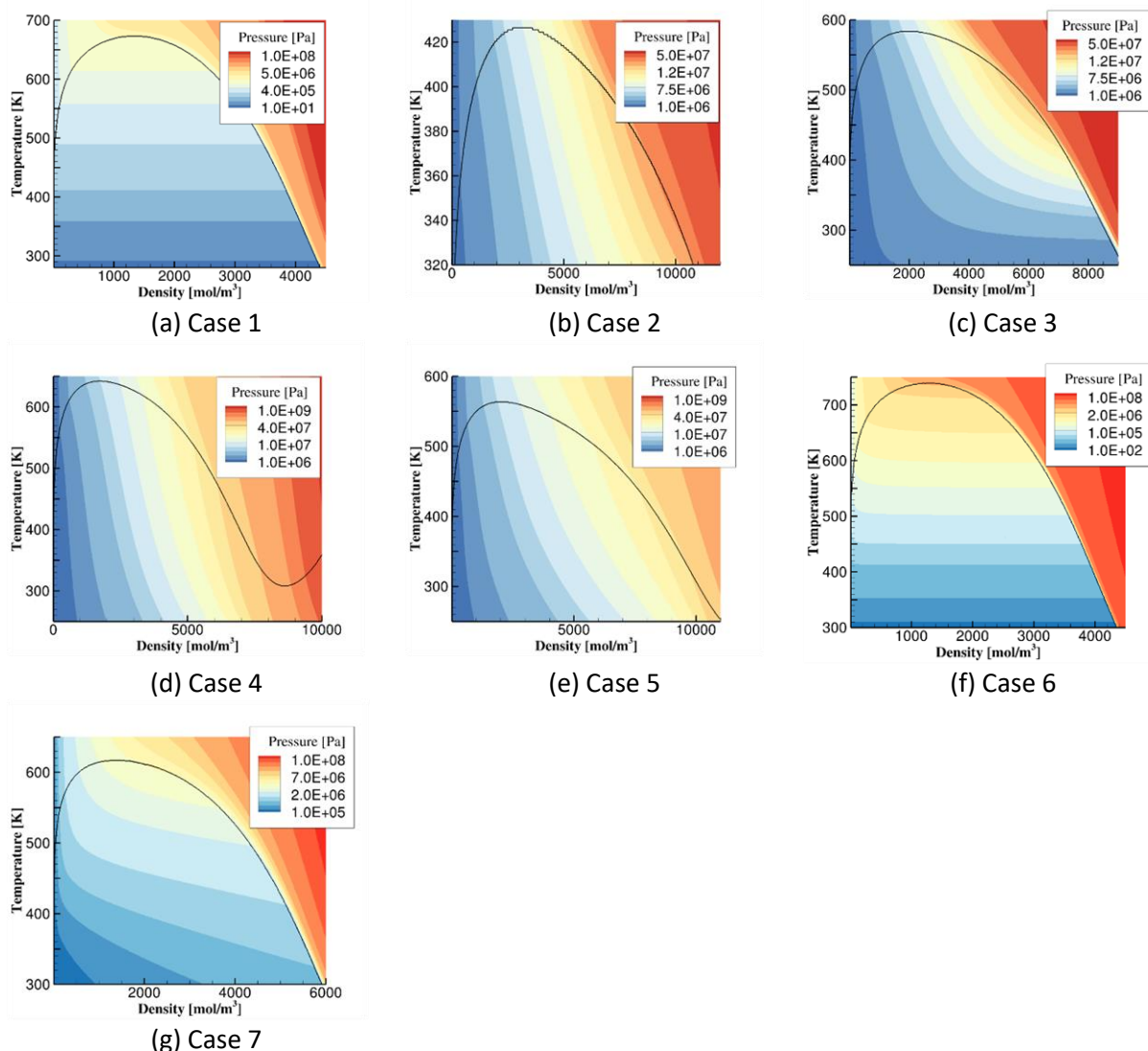


Figure 1. Pressure field for all cases studied in the paper, the black curve draws the saturation line. The colour scale is unique for every figure.

444 Figure 1 shows the pressure field for every case, marking with a black curve the saturation line.
 445 Depending on the components and composition, the pressure field varies significantly. Cases 1 and 6,
 446 those which are meant to model Diesel fuel, show similar horizontal isobaric lines when in the VLE
 447 region, where the PT-VLE algorithm is known to fail. Case 1 shows isobaric-isothermal phase transition
 448 by definition, as it is a single component. Case 6, the 8-component mixture, shows a similar trend due to
 449 the similarity between the components, although the small differences among them can be seen close
 450 to the dew curve, where the isobars bend upwards. Cases 2, 4 and 5 show isobars with significant slope
 451 which isobaric vapor-liquid transition comes with a massive decrease in temperature, typical of mixtures

452 exhibiting extremely different phase transition properties. For instance, from Case 2 the critical
453 temperature of pentane is close to 2.5 times than that of methane, while more obviously in Case 4 the
454 critical temperature of dodecane is more than 5 times higher than that of dodecane. Case 3 shows an
455 intermediate field between Cases 1 and 2, where while at high temperatures the slope is sufficiently
456 pronounced, at low temperatures and high densities the isobars become progressively flat, where the
457 PT-VLE problem is expected to start failing. Regarding the 50-component hydrocarbon mixture, the
458 isobars show significant slope as there are both very light and very heavy hydrocarbons, for instance
459 methane and octadecane.

460 **3.2 Vapor volume Fraction Field**

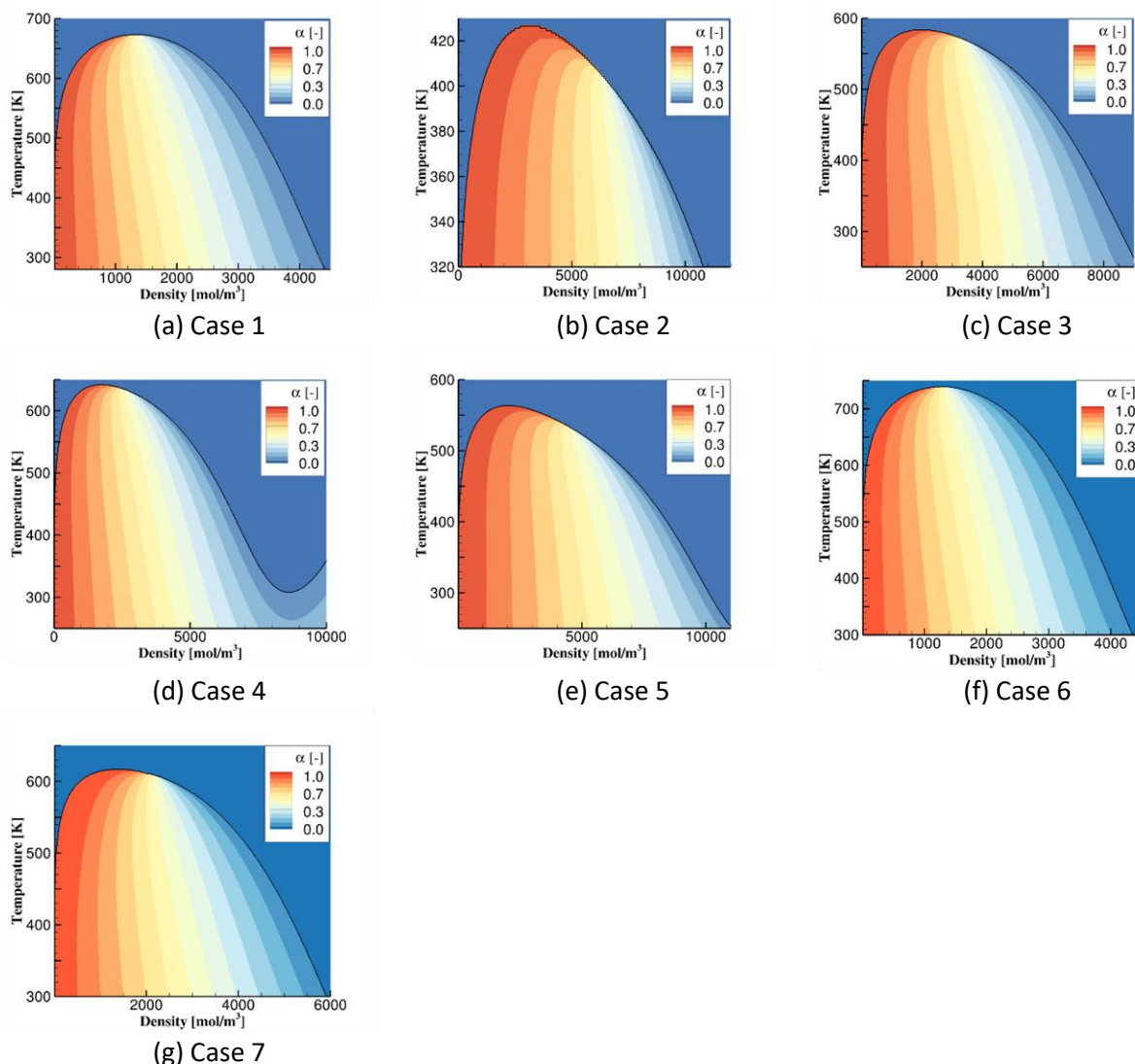


Figure 2. Vapor volume fraction field for all cases studied in the paper, the black curve draws the saturation line. The colour scale is the same on every figure.

461 Figure 2 shows the vapor volume fraction field for every case, marking with a black curve the
 462 saturation line. Cases 1 and 6 show the typical vapor volume fraction field for every single component,
 463 where the isolines converge at the critical point, being in this case the maximum temperature and
 464 pressure at which a two-phase state can be found. On the rest of cases, the critical point is not located
 465 on the maximum two-phase temperature or pressure, but on a lower value. This phenomenon gives rise
 466 to the retrograde vaporisation⁵², which accounts for the anomalous isothermal vaporisation of the
 467 mixture when the pressure is increased. Case 4, in addition, shows at 320K a liquid-liquid critical point,

468 where the equilibrium pressure is higher than 100MPa, clearly seen on the change in curvature of the
469 saturation curve.

470 **3.3 Flash iterations until convergence**

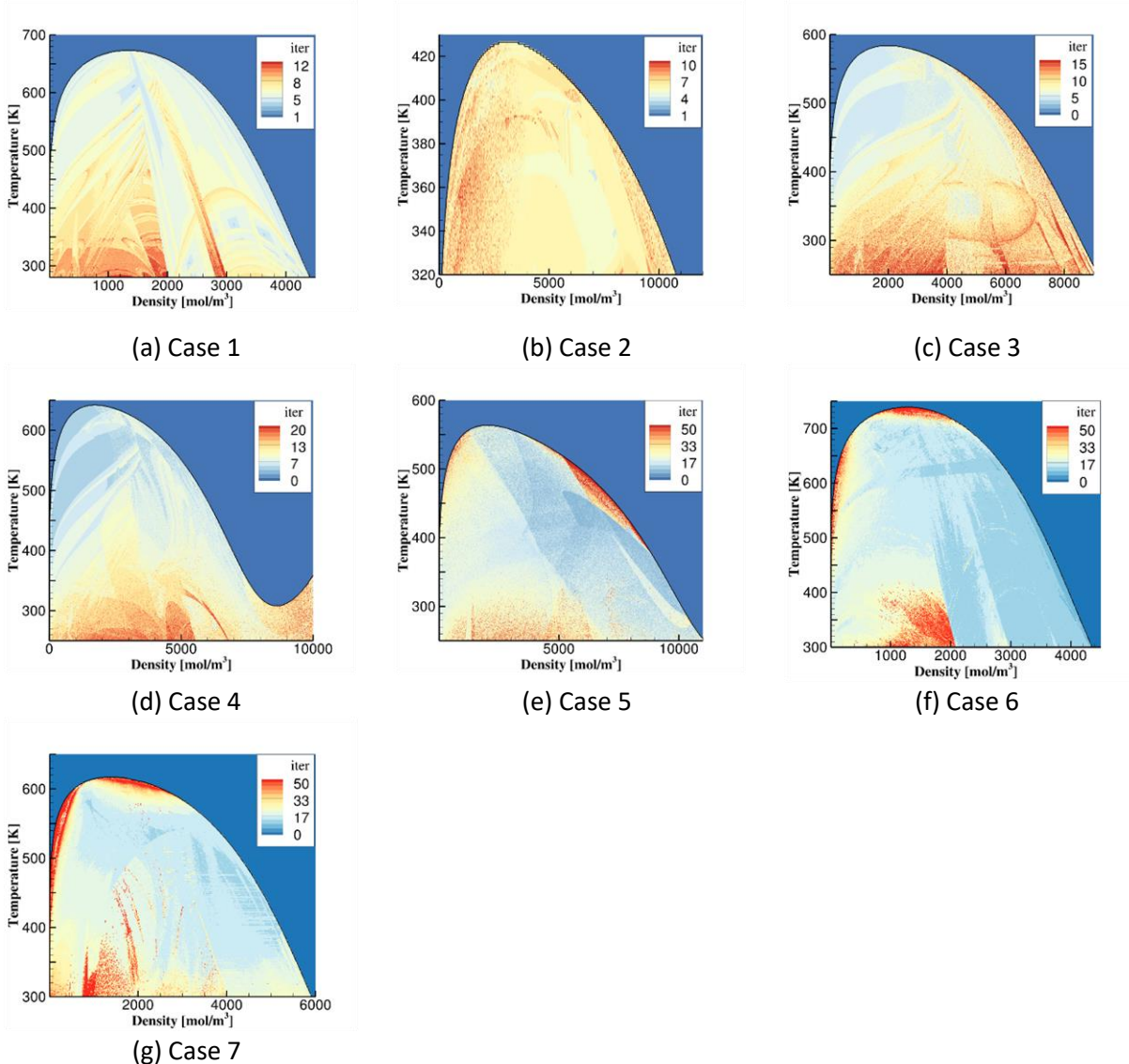


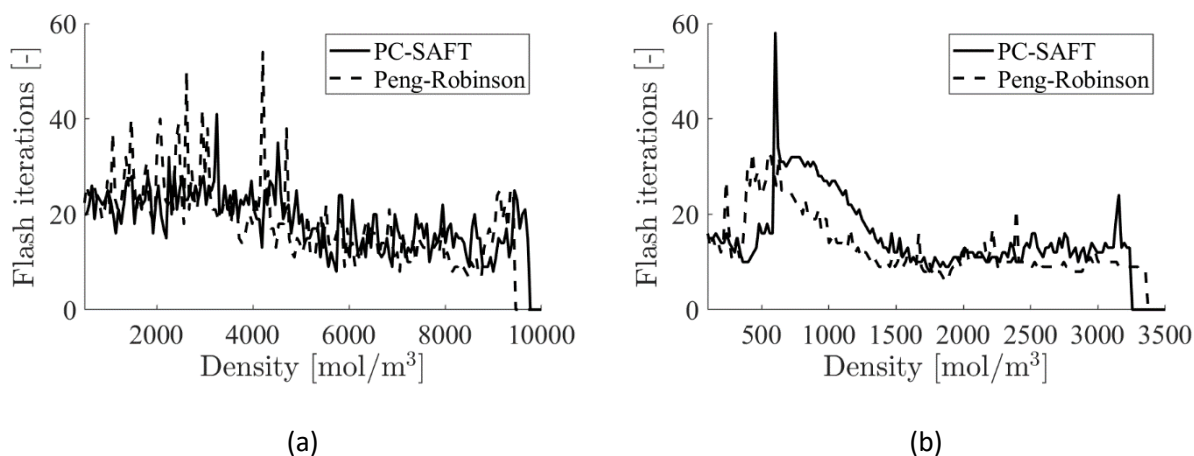
Figure 3. Flash iterations field for all cases studied in the paper, the black curve draws the saturation line. The colour scale is unique for every figure.

471 Figure 3 shows the number of flash iterations needed for convergence using the NVL-algorithm for
 472 every case, marking with a black curve the saturation line. Case 1 shows a reasonably homogeneous
 473 distribution, with maximum number of iterations of 10 at low temperatures and intermediate densities.
 474 The distribution of Case 2 iterations is as homogeneous as in Case 1, with a maximum iteration number
 475 of 10. For Case 3, the highest numbers are localised at temperatures lower than 350K and close to the
 476 bubble-point curve, where the number of iterations reach 15. Regarding Case 4, the higher number of
 477 iterations are found at temperatures lower than 350K and at densities higher than 9,000mol/m³, where
 478 the calculated equilibrium pressure reaches 1,000MPa. For the 4-component mixture in Case 5, more

479 than 50 iterations are needed along to the bubble point curve at high temperatures. High number of
480 iterations are also observed for temperatures lower than 300K and close to the dew-point curve at high
481 temperatures. Overall, at high temperatures the phase change needs a particularly high number of
482 iterations for convergence. The 8-component surrogate in Case 6 the maximum number of iterations,
483 which may reach 100, are found close to the critical point and at high temperatures close to the dew-
484 point curve. For the 50-component hydrocarbon mixture, the number of iterations grow considerably
485 compared with the previous cases, where the threshold of 150 iterations is reached again at the critical
486 point and the dew curve, in addition to localised high number of iterations at $1,000\text{mol/m}^3$ and
487 temperatures lower than 350K.

488 3.4 Performance comparison against Peng Robinson EoS

489 The performance of the algorithm can be influenced significantly by the chosen equation of state, as
490 every iteration needs the calculation of many properties and its derivatives for the two phases. The use
491 of PC-SAFT EoS has been already reported to increase the computational time needed for a single
492 equilibrium calculation with respect to Peng Robinson⁵³. Previous works, using a PT-VLE calculation,
493 have obtained differences in CPU time of 2-3 times between the Peng Robinson EoS and PC-SAFT EoS⁴⁰
494 for a variety of mixtures. For some mixtures, even, the computational time was found smaller for the
495 original PC-SAFT than for the cubic EoS. However, von Solms⁴⁰ estimated that the CPU time needed for
496 the calculation of all the derivatives involved in the PT-VLE was 4-5 times higher than for the SRK EoS,
497 using the simplified PC-SAFT for a mixture of 15 components. The simplified PC-SAFT is known to be
498 significantly more efficient in VLE calculations as some of the terms of the original version become
499 composition-independent. Therefore, the difference between cubic EoS and the PC-SAFT is expected to
500 be higher than 4-5 times, even if the number of function evaluations is similar.



501 Figure 4. Flash iterations needed for Cases 5 and 6 at 300K using Peng-Robinson and PC-SAFT as
502 Equations of State at 300K.

503 Figure 4 shows two performance comparisons for Cases 5 (4 component mixture) and 6 (8 component
504 mixture) regarding the iterations needed for calculating the equilibrium at 300K for a range of densities,
505 using both Peng Robinson and PC-SAFT EoS. Flash iterations are both initialized from a previous stability
506 analysis. As shown, for the 4-component mixture the iterations needed are quite similar for both

507 Equations of State, apart from particular conditions at which the cubic equation seems to spike. Overall,
 508 the iterations needed at lower densities than 5000mol/m³ are higher than those at higher densities. For
 509 the 8-component surrogate, the number of iterations needed at low densities are significantly higher for
 510 PC-SAFT, although at densities higher than 1500mol/m³ the convergence is achieved in a similar number
 511 of iterations.

EoS	Case 1	Case 2	Case 3	Case 4	Case 5	Case 6	Case 7
PC-SAFT	629.79	1340.6	1143.8	1059.4	1878.1	13996	363270
Peng Robinson	156.25	182.62	191.98	210.94	250.31	937.53	10332
Ratio	4.03	7.34	5.96	5.02	7.5	14.9	35.16

512 Table 4: Computational time in μ s, per single VLE calculation, needed for all cases using Peng Robinson
 513 and PC-SAFT. The last row shows the ratio between both CPU times.

514 Table 4 shows the computational time, per VLE calculation, needed for all cases using both Peng
 515 Robinson and PC-SAFT EoS. Results indicate a significant difference between both EoS, which increases
 516 with the number of components. While for a single component the CPU time for PC-SAFT is about 4
 517 times higher than for Peng-Robinson, for two components it grows to about 6 and up to 15 for the 8-
 518 component surrogate of case 6. An extreme case is seen for case 7, where the computational time
 519 needed to calculate the VLE for a 50-component mixture increases to 35. These differences can be
 520 explained due to the high dependence on composition of the PC-SAFT EoS, which increases the number
 521 of calculations needed for the derivatives exponentially. The reader may acknowledge the extent of the
 522 derivations in the complete formulation of the algorithm found in the Supplementary Information. This
 523 can be also seen in Table 5, where the computational time per single calculation of the derivatives is
 524 shown. The range in temperature and density per case is the same as in previous chapters. As seen, the
 525 difference between the CPU time of Peng Robinson and PC-SAFT grows with the number of components
 526 in a similar fashion than for the complete VLE calculations. Discrepancies between the single EoS and
 527 complete VLE calculations can be explained because of differences in the number of iterations needed
 528 for the convergence, which is not necessarily the same, although similar as already seen in Figure 4.

529

EoS	Case 1	Case 2	Case 3	Case 4	Case 5	Case 6	Case 7
PC-SAFT	8.844	13.37	13.70	14.66	31.20	100.0	25380
Peng Robinson	1.800	2.323	2.341	2.342	3.421	7.046	58.75
Ratio	4.91	5.76	5.84	6.25	9.12	14.19	43.2

530 Table 5: Computational time in μs , per single calculation of all the needed derivatives, for all cases using
531 Peng Robinson and PC-SAFT. The last row shows the ratio between both CPU times.

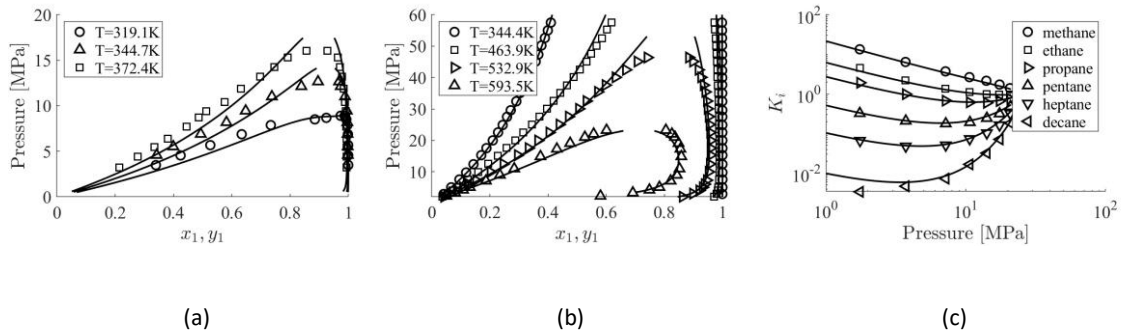
532

533 These results show why when computational power is the main restriction in simulations, past works
534 tend to choose the Peng-Robinson over more accurate EoS such as the PC-SAFT. For instance, in
535 Computational Fluid Dynamics, equilibrium calculations may be needed in more than 1 million cells per
536 timestep, making the EoS choice the main decision criterion regarding the trade-off between accuracy
537 and computational efficiency.

538 **3.5 Validation against experiments**

539 Figure 6 shows validation cases to assess the accuracy of the model when compared to experimental
 540 data. The data was collected and compared for Case 2⁵⁴, Case 4⁵⁵ and the Y8 synthetic mixture⁵¹. The Y8
 541 mixture is composed of 6 components with composition: 0.8097 methane, 0.0566 ethane, 0.0306
 542 propane, 0.0457 n-pentane, 0.0330 n-heptane and 0.0244 n-decane. The binary interaction parameters
 543 were set to 0 for the Y8 mixture. As it can be seen, there exists good agreement for every case using the
 544 corresponding binary interaction parameters. The first two figures show the typical binary phase
 545 diagram at different constant temperatures, while the first figure shows the equilibrium constants for
 546 every component in the mixture at fixed temperature.

547



550 Figure 6: Predicted vapor-liquid equilibrium compared with experimental data for (a) Case 2, (b) Case 4
 551 and (c) the Y8 mixture [37].

552 Table 5 shows the Average Absolute Deviation (AAD [%]) of the calculations with respect to the
 553 experimental values for the above cases and it is defined as:

$$554 \quad AAD[\%] = \frac{100}{N_p} \sum_i^{N_p} \left| \frac{(x_i, y_i)^{exp} - (x_i, y_i)^{calc}}{(x_i, y_i)^{exp}} \right| \quad (50)$$

555 Where N_p is the number of compared experimental data points.

556

557

	Case 2	Case 4	Y8 Mixture
<i>AAD</i> [%]	2.7901	0.9281	3.6289

558 Table 5: Average Absolute Deviation (AAD [%]) of the three cases shown in Figure 6.

559 As observed in the table, the agreement with experiments is good even for the 6-component mixture,
560 where the average deviation is lower than 4%. However, it is necessary to notice that this agreement is
561 significantly dependent on the binary interaction parameter k_{ij} which is obtained by fitting with
562 experimental VLE data.

563

564 **4 Conclusions**

565 In this study, the PC-SAFT EoS was used for Vapor Equilibrium calculation at specified composition,
566 density and temperature. The presented algorithm was tested on several cases of both single and
567 multicomponent substances. The calculation utilised the Newton iterations to reach the global minimum
568 of the Helmholtz free energy in two stages, namely stability analysis and flash. As a result, the pressure
569 of the fluid and the compositions of both the liquid and vapor phases were calculated. The reliability of
570 two different methods for the flash stage, one based in number of moles and volume (NVL) and another
571 based in the logarithm of the equilibrium constants (lnK), were evaluated in terms of both iterations and
572 computer time needed to reach convergence.

573 Results showed that although the lnK method needs less iterations until convergence, the total
574 computational time needed is considerably longer. This difference in computational time is caused
575 during the calculation of density in the pressure equality condition, as it needs to be satisfied iteratively.
576 The NVL method does not need to satisfy this condition at every iteration, therefore no inner iterative
577 loops are needed, and faster convergence was obtained. Moreover, the lnK method cannot be used for
578 single components, as its value is unity during all iterations, and it fails continuously for mixtures with
579 similar components, as the 8-component Diesel surrogate studied in Case 6. A performance comparison
580 was obtained against the Peng-Robinson EoS, showing a substantial decrease in computational time
581 when using the cubic compared to the molecular based EoS. Validation against experiments show good
582 agreement of the numerical model.

583 Future work should be headed towards more complex mixtures, resourcing to the latest applications
584 of PC-SAFT introducing associating⁵⁶, multipolar^{57 58} and/or aqueous ionic liquid solutions⁵⁹, as the
585 accuracy of this molecular-based EoS is of great value for academic and industrial applications.

586 **5 Acknowledgements**

587 This project has received funding from the European Union Horizon-2020 Research and
588 Innovation Programme. Grant Agreement No 675528.

589 The authors would like to thank the invaluable help of Dr. Mikyška's group, particularly Tomáš Smejkal,
590 for sharing their VLE data and continuous assistance for the completion of this article.

591 **6 Nomenclature**

A	Helmholtz free energy	Greek letters	
z	pressure	α	transformed stability variables
ρ	molar density	σ	segment diameter
T	temperature	δ_{ij}	Kronecker delta
E	modified Cholesky diagonal matrix	λ	step length
P	permutation matrix	ϵ	energy parameter
P	pressure	ϵ	variables vector
p	search direction	ω	acentric factor
M	Cholesky lower triangular matrix	β	Vapor fraction
B	Hessian submatrix	Subscripts	
C	Hessian submatrix	i, j	component index
D	Hessian submatrix	c	critical property
g	gradient vector	sat	saturation
H	Hessian matrix	max	maximum
I	identity matrix	Superscripts	
R_g	universal gas constant	$*$	feed property
x_i	mole fraction of component i in a phase	v	vapor phase
z_i	mole fraction of component i in the feed	l	liquid phase
Z	reducing matrix	(k)	iteration number
nc	number of components	$'$	trial phase
n_i	number of moles of component i	eq	equilibrium
f_i	fugacity of component i	res	residual contribution
m	number of segments	id	ideal contribution
k_B	Boltzmann constant		
K_i	equilibrium constant		
\tilde{u}	intermediate Cholesky vector		
u	intermediate Cholesky vector		
V	volume		
TPD	Tangent Plane Distance		

592

593

594 **7 References**

- 595 1. Gross, J.; Sadowski, G., Perturbed-chain SAFT: An equation of state based on a perturbation
596 theory for chain molecules. *Industrial & engineering chemistry research* **2001**, *40*, 1244-1260.
- 597 2. Wertheim, M. S., Fluids with highly directional attractive forces. I. Statistical thermodynamics.
598 *Journal of statistical physics* **1984**, *35*, 19-34.
- 599 3. Wertheim, M. S., Fluids with highly directional attractive forces. II. Thermodynamic perturbation
600 theory and integral equations. *Journal of statistical physics* **1984**, *35*, 35-47.
- 601 4. Wertheim, M. S., Fluids with highly directional attractive forces. III. Multiple attraction sites.
602 *Journal of statistical physics* **1986**, *42*, 459-476.
- 603 5. Wertheim, M. S., Fluids with highly directional attractive forces. IV. Equilibrium polymerization.
604 *Journal of statistical physics* **1986**, *42*, 477-492.
- 605 6. De Villiers, A.; Schwarz, C.; Burger, A.; Kontogeorgis, G., Evaluation of the PC-SAFT, SAFT and
606 CPA equations of state in predicting derivative properties of selected non-polar and hydrogen-bonding
607 compounds. *Fluid Phase Equilibria* **2013**, *338*, 1–15.
- 608 7. Leekumjorn, S.; Krejbjerg, K., Phase behavior of reservoir fluids: Comparisons of PC-SAFT and
609 cubic EOS simulations. *Fluid Phase Equilibria* **2013**, *359*, 17–23.
- 610 8. Peng, D.-Y.; Robinson, D. B., A new two-constant equation of state. *Industrial & Engineering*
611 *Chemistry Fundamentals* **1976**, *15*, 59-64.
- 612 9. Soave, G., Equilibrium constants from a modified Redlich-Kwong equation of state. *Chemical*
613 *Engineering Science* **1972**, *27*, 1197-1203.
- 614 10. Yan, W.; Varzandeh, F.; Stenby, E. H., PVT modeling of reservoir fluids using PC-SAFT EoS and
615 Soave-BWR EoS. *Fluid Phase Equilibria* **2015**, *386*, 96-124.
- 616 11. Burgess, W. A.; Tapriyal, D.; Morreale, B. D.; Soong, Y.; Baled, H. O.; Enick, R. M.; Wu, Y.;
617 Bamgbade, B. A.; McHugh, M. A., Volume-translated cubic EoS and PC-SAFT density models and a free
618 volume-based viscosity model for hydrocarbons at extreme temperature and pressure conditions. *Fluid*
619 *Phase Equilibria* **2013**, *359*, 38–44.
- 620 12. Schou Pedersen, K.; Hasdbjerg, C. In *PC-SAFT equation of state applied to petroleum reservoir*
621 *fluids*, SPE Annual Technical Conference and Exhibition, 2007.
- 622 13. Gord, M. F.; Roozbahani, M.; Rahbari, H. R.; Hosseini, S. J. H., Modeling thermodynamic
623 properties of natural gas mixtures using perturbed-chain statistical associating fluid theory. *Russian*
624 *Journal of Applied Chemistry* **2013**, *86*, 867–878.
- 625 14. Panuganti, S. R.; Vargas, F. M.; Gonzalez, D. L.; Kurup, A. S.; Chapman, W. G., PC-SAFT
626 characterization of crude oils and modeling of asphaltene phase behavior. *Fuel* **2012**, *93*, 658–669.
- 627 15. Zúñiga-Hinojosa, M. A.; Justo-García, D. N.; Aquino-Olivos, M. A.; Román-Ramírez, L. A.; García-
628 Sánchez, F., Modeling of asphaltene precipitation from n-alkane diluted heavy oils and bitumens using
629 the PC-SAFT equation of state. *Fluid Phase Equilibria* **2014**, *376*, 210–224.
- 630 16. Arya, A.; Liang, X.; Von Solms, N.; Kontogeorgis, G. M., Modeling of Asphaltene Onset
631 Precipitation Conditions with Cubic Plus Association (CPA) and Perturbed Chain Statistical Associating
632 Fluid Theory (PC-SAFT) Equation of States.
- 633 17. Nascimento, F. P.; Costa, G. M. N.; Melo, S. A. B. V., A comparative study of CPA and PC-SAFT
634 equations of state to calculate the asphaltene onset pressure and phase envelope. *Fluid Phase Equilibria*
635 **2019**, *494*, 74-92.
- 636 18. Kontogeorgis, G. M.; Folas, G. K., *Thermodynamic models for industrial applications: from*
637 *classical and advanced mixing rules to association theories. Appendix A*. John Wiley & Sons: 2009.
- 638 19. Zhao, Y.; Dong, X.; Zhong, Q.; Zhang, H.; Li, H.; Shen, J.; Gong, M., Modeling Vapor Liquid
639 Phase Equilibrium for C_xH_y C_xH_yF_z Using Peng–Robinson and Perturbed-Chain SAFT. *Industrial &*
640 *Engineering Chemistry Research* **2017**, *56*, 7384-7389.
- 641 20. Vidal, A.; Rodriguez, C.; Koukouvinis, P.; Gavaises, M.; McHugh, M. A., Modelling of Diesel fuel
642 properties through its surrogates using Perturbed-Chain, Statistical Associating Fluid Theory.
643 *International Journal of Engine Research* **2018**, 146808741880171.

- 644 21. Carneiro, A. P.; Held, C.; Rodríguez, O.; Sadowski, G.; Macedo, E. A., Solubility of Sugars and
645 Sugar Alcohols in Ionic Liquids: Measurement and PC-SAFT Modeling. *The Journal of Physical Chemistry*
646 *B* **2013**, *117*, 9980-9995.
- 647 22. Abolala, M.; Peyvandi, K.; Varaminian, F.; Hashemianzadeh, S. M., A comprehensive description
648 of single-phase and VLE properties of cryogenic fluids using molecular-based equations of state. *Fluid*
649 *Phase Equilibria* **2019**, *494*, 143-160.
- 650 23. Diamantonis, N. I.; Boulougouris, G. C.; Mansoor, E.; Tsangaris, D. M.; Economou, I. G.,
651 Evaluation of Cubic, SAFT, and PC-SAFT Equations of State for the Vapor–Liquid Equilibrium Modeling of
652 CO₂ Mixtures with Other Gases. *Industrial & Engineering Chemistry Research* **2013**, *52*, 3933-3942.
- 653 24. Rodriguez, C.; Koukouvinis, P.; Gavaises, M., Simulation of supercritical diesel jets using the PC-
654 SAFT EoS. *The Journal of Supercritical Fluids* **2019**, *145*, 48-65.
- 655 25. Vidal, A.; Koukouvinis, P.; Gavaises, M. In *On the effect of realistic multicomponent diesel*
656 *surrogates on cavitation and in-nozzle flow*, IMechE, 2018.
- 657 26. Polívka, O.; Mikyška, J., Compositional modeling in porous media using constant volume flash
658 and flux computation without the need for phase identification. *Journal of Computational Physics* **2014**,
659 *149*-169.
- 660 27. Jindrová, T., *Computational methods in thermodynamics of multicomponent mixtures*. Master
661 degree thesis, Czech Technical University in Prague: 2013.
- 662 28. Michelsen, M. L., The isothermal flash problem. Part I. Stability. *Fluid Phase Equilibria* **1982**, *9*, 1-
663 19.
- 664 29. Nichita, D. V.; de-Hemptinne, J.-C.; Gomez, S., Isochoric Phase Stability Testing for Hydrocarbon
665 Mixtures. *Petroleum Science and Technology* **2009**, *27*, 2177-2191.
- 666 30. Levy, A. V.; Gómez, S., The tunneling method applied to global optimization. *Numerical*
667 *optimization* **1985**, *1981*, 213-244.
- 668 31. Mikyška, J.; Firoozabadi, A., A new thermodynamic function for phase-splitting at constant
669 temperature, moles, and volume. *AIChE Journal* **2010**, *57*, 1897-1904.
- 670 32. Jindrová, T.; Mikyška, J., General algorithm for multiphase equilibria calculation at given volume,
671 temperature, and moles. *Fluid Phase Equilibria* **2015**, *393*, 7-25.
- 672 33. Nichita, D. V., New unconstrained minimization methods for robust flash calculations at
673 temperature, volume and moles specifications. *Fluid Phase Equilibria* **2018**, *466*, 31-47.
- 674 34. Paterson, D.; Michelsen, M. L.; Yan, W.; Stenby, E. H., Extension of modified RAND to
675 multiphase flash specifications based on state functions other than (T,P). *Fluid Phase Equilibria* **2018**,
676 *458*, 288-299.
- 677 35. Tang, X.; Gross, J., Renormalization-group corrections to the perturbed-chain statistical
678 associating fluid theory for binary mixtures. *Industrial and Engineering Chemistry Research* **2010**, 9436-
679 9444.
- 680 36. Bymaster, A.; Emborsky, C.; Dominik, A.; Chapman, W. G., Renormalization-group corrections
681 to a perturbed-chain statistical associating fluid theory for pure fluids near to and far from the critical
682 region. *Industrial and Engineering Chemistry Research* **2008**, 6264-6274.
- 683 37. García-Sánchez, F.; Schwartzentruber, J.; Ammar, M. N.; Renon, H., Modeling of multiphase
684 liquid equilibria for multicomponent mixtures. *Fluid phase equilibria* **1996**, *121*, 207-225.
- 685 38. Schnabel, R. B.; Eskow, E., A Revised Modified Cholesky Factorization Algorithm. *SIAM Journal on*
686 *Optimization* **1999**, *9*, 1135-1148.
- 687 39. Jindrová, T.; Mikyška, J., Fast and robust algorithm for calculation of two-phase equilibria at
688 given volume, temperature, and moles. *Fluid Phase Equilibria* **2013**, *353*, 101-114.
- 689 40. von Solms, N.; Michelsen, M. L.; Kontogeorgis, G. M., Computational and Physical Performance
690 of a Modified PC-SAFT Equation of State for Highly Asymmetric and Associating Mixtures. *Industrial &*
691 *Engineering Chemistry Research* **2003**, 1098-1105.
- 692 41. Nocedal, J.; Wright, S., *Numerical Optimization*. Springer New York: 2006.
- 693 42. Fletcher, R., *Practical methods of optimization*. John Wiley & Sons: 2013.
- 694 43. Baker, L. E.; Pierce, A. C.; Luks, K. D., Gibbs Energy Analysis of Phase Equilibria. *Society of*
695 *Petroleum Engineers Journal* **1982**, *22*, 731-742.

- 696 44. Mikyška, J.; Firoozabadi, A., Investigation of mixture stability at given volume, temperature, and
697 number of moles. *Fluid Phase Equilibria* **2012**, *321*, 1-9.
- 698 45. Nichita, D. V., Fast and robust phase stability testing at isothermal-isochoric conditions. *Fluid*
699 *Phase Equilibria* **2017**, *447*, 107-124.
- 700 46. Wilson, G. M. In *A modified Redlich-Kwong equation of state, application to general physical*
701 *data calculations*, 65th National AIChE Meeting, Cleveland, OH, 1969; p 15.
- 702 47. Privat, R.; Gani, R.; Jaubert, J. N., Are safe results obtained when the PC-SAFT equation of state
703 is applied to ordinary pure chemicals? *Fluid Phase Equilibria* **2010**, 76-92.
- 704 48. Press, W. H.; Flannery, B. P.; Teukolsky, S. A.; Vetterling, W. T.; Gould, H., Numerical Recipes,
705 The Art of Scientific Computing. *American Journal of Physics* **1987**, *55*, 90-91.
- 706 49. Dahms, R. N.; Manin, J.; Pickett, L. M.; Oefelein, J. C., Understanding high-pressure gas-liquid
707 interface phenomena in Diesel engines. *Proceedings of the Combustion Institute* **2013**, *34*, 1667-1675.
- 708 50. Mueller, C. J.; Cannella, W. J.; Bays, J. T.; Bruno, T. J.; DeFabio, K.; Dettman, H. D.; Gieleciak,
709 R. M.; Huber, M. L.; Kweon, C.-B.; McConnell, S. S., Diesel surrogate fuels for engine testing and
710 chemical-kinetic modeling: Compositions and properties. *Energy & Fuels* **2016**, *30*, 1445-1461.
- 711 51. Yarborough, L., Vapor-liquid equilibrium data for multicomponent mixtures containing
712 hydrocarbon and nonhydrocarbon components. *Journal of Chemical & Engineering Data* **1972**, *17*, 129-
713 133.
- 714 52. Kuenen, J. P., On Retrograde Condensation and the Critical Phenomena of Two Substances.
715 *Commun. Phys. Lab U. Leiden* **1892**.
- 716 53. Liang, X., On the efficiency of PT Flash calculations with equations of state. *Computer Aided*
717 *Chemical Engineering* **2018**, 859-864.
- 718 54. Chu, T.-C.; Chen, R. J. J.; Chappellear, P. S.; Kobayashi, R., Vapor-liquid equilibrium of methane-
719 n-pentane system at low temperatures and high pressures. *Journal of Chemical & Engineering Data*
720 **1976**, *21*, 41-44.
- 721 55. Garcia-Cordova, T.; Justo-Garcia, D. N.; Garcia-Flores, B. E.; Garcia-Sanchez, F., Vapor-Liquid
722 Equilibrium Data for the Nitrogen - Dodecane System at Temperatures from (344 to 593) K and at
723 Pressures up to 60 MPa. *Journal of Chemical & Engineering Data* **2011**, *56*, 1555-1564.
- 724 56. Gross, J.; Sadowski, G., Application of the perturbed-chain SAFT equation of state to associating
725 systems. *Industrial and Engineering Chemistry Research* **2002**, 5510-5515.
- 726 57. Gross, J.; Vrabec, J., An equation-of-state contribution for polar components: Dipolar molecules.
727 *AIChE Journal* **2006**, 1194-1204.
- 728 58. Gross, J., An equation-of-state contribution for polar components: Quadrupolar molecules.
729 *AIChE Journal* **2005**, 2556-2568.
- 730 59. Shahriari, R.; Dehghani, M. R.; Behzadi, B., Thermodynamic modeling of aqueous ionic liquid
731 solutions using PC-SAFT equation of state. *Industrial and Engineering Chemistry Research* **2012**, 10274-
732 10282.

733